NaLaF 4 :Pr 3+ ,Yb 3+ , an efficient blue to near infra-red quantum cutter

A Guille, A Pereira, B Moine

APL Materials

$NaLaF_4:Pr^{3+},Yb^{3+}$, an efficient blue to near infra-red quantum cutter

Cite as: APL Mater. **1**, 062106 (2013); https://doi.org/10.1063/1.4843455
Submitted: 26 July 2013 . Accepted: 26 November 2013 . Published Online: 10 December 2013

A. Guille, A. Pereira, and B. Moine

$NaLaF_4:Pr^{3+},Yb^{3+}$, an efficient blue to near infra-red quantum cutter

A. Guille, A. Pereira, and B. Moine[a]
Université Lyon 1, CNRS UMR 5306, Institut Lumière Matière, Université de Lyon, F-69622 Villeurbanne, France

(Received 26 July 2013; accepted 26 November 2013; published online 10 December 2013)

In order to reduce the thermalization losses in solar cells, down-conversion of blue photons into near infra-red photons is a promising solution. In the present paper, we analyse the energy transfer processes between Pr^{3+} and Yb^{3+} in $NaLaF_4$ and we show that an efficient quantum-cutting process occurs. Nevertheless, we also show that a back transfer from Yb^{3+} toward the $^1G_4$ level of Pr^{3+} ion leading to emission beyond 1 μm reduces the potentiality of this material as a quantum cutter for Si solar cells. [http://dx.doi.org/10.1063/1.4843455]

Thermalization of electron-hole pairs created by high energy photons is responsible for the poor yield of solar cells in the blue range of the solar spectrum.[1] In order to improve this "blue" yield one can adapt the incident solar spectrum by deposition of a thin layer of a so called quantum-cutting material in front of the solar cell.[2–4] Each incident blue photon could thus be converted into two near infra-red photons, both able to generate an electron-hole pair. A process of quantum-cutting between rare-earth ions has been proposed and recently reviewed.[5,6] Such a mechanism was observed, for example, within the couple Pr^{3+}–Yb^{3+} in SrF_2.[7] As shown in Fig. 1, after the absorption of a blue photon by the Pr^{3+} ion by the ^3P_j levels, a two-step relaxation Pr^{3+}:$\{^3P_0 \rightarrow {}^1G_4, {}^1G_4 \rightarrow {}^3H_4\}$ $\rightarrow 2 \times Yb^{3+}$:$\{^2F_{7/2} \rightarrow {}^2F_{5/2}\}$ can occur, leading to the emission of two infra-red photons by the two excited Yb^{3+} ions.[8]

In order to be very efficient, a quantum cutter material must have the lower phonon energy as possible. Thus, fluoride materials which have quite low maximum phonon energy are good host matrix for such application. Serrano *et al.* have studied (Pr^{3+}, Yb^{3+}) couple and demonstrated that the first energy transfer (a) in Fig. 1 is very efficient in CaF_2 crystals.[9] Here, we present results obtained in $NaLaF_4$ (NLF) co-doped with the same ion couple.

Pr^{3+}–Yb^{3+} co-doped NLF was synthesized by solid state reaction, after grinding and mixing NaF(99.99% purity), LaF_3(99.9% purity) in stoichiometric proportions. All the raw materials were from Alfa Aesar company. The samples were sintered at 600 °C for 3×6 h (every 6 h samples were ground and mixed again) under a reducing CF_4 atmosphere in order to avoid any O_2 pollution. PrF_3(99.9% purity) and YbF_3(99.9% purity) were added in order to dope NLF with Pr^{3+} and Yb^{3+}, respectively (doping rates are given in at. %). For an efficient quantum cutting process, it is necessary to have at least twice as much Yb^{3+} than Pr^{3+}. On the other hand, concentrations must not be too high in order to avoid concentration quenching which could reduce the final fluorescence efficiency. Thus, samples have been doped by 0.5 at. % Pr^{3+} and 0, 1, 5 and 7 at. % Yb^{3+}. The phase purity of the samples was controlled by X-ray diffraction using a Bruker D8 Advance diffractometer with Cu Kα radiation. The diffractogramms were recorded from $2\Theta = 10°$ to 70° with a 0.021° step size and a counting time of 4 s per step. The fluorescence spectra measurements were performed at room temperature with a CCD sensor associated with a monochromator TRIAX 190 from Jobin-Yvon

[a]Author to whom correspondence should be addressed. Electronic mail: bernard.moine@univ-lyon1.fr

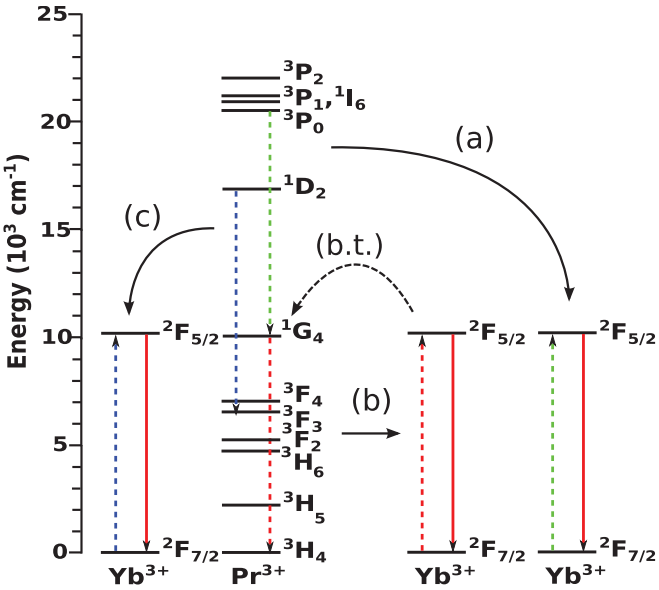

FIG. 1. Principle of quantum-cutting with Pr^{3+} and Yb^{3+}. (a)–(c) are three possible mechanisms of energy transfer from Pr^{3+} toward Yb^{3+} and (b.t.) is the back-transfer mechanism from Yb^{3+} to Pr^{3+}.

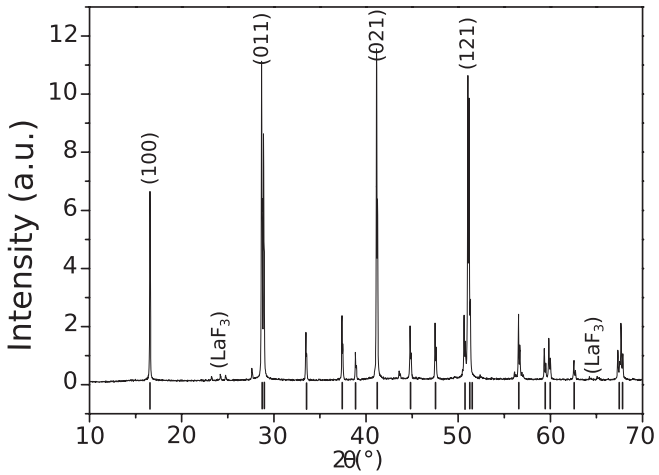

FIG. 2. XRD spectrum of $NaLaF_4$. Vertical lines correspond to the related JCPDS card no. 01-075-1923. Main pics are indexed.

(3.53 nm/mm, the width of the entrance slit was set at 200 μm) using a tunable pulsed laser EKSPLA NT340 as excitation source. A 450 W Xe lamp associated with a monochromator GEMINI 180 (2.1 nm/mm, the width of slits was 1 mm) from Jobin-Yvon was used to perform excitation spectra. Fluorescence decay was recorded with a single channel analyser SR430 from Stanford company.

The diffractogramm depicted in Fig. 2 exhibits a series of diffraction peaks corresponding to a pure $NaLaF_4$ phase (only a few very residual peaks, around 25° and 65°, corresponding to LaF_3 phase can be seen). $NaLaF_4$ is a high efficiency material for luminescence due to small effective phonon energy (~290 cm^{-1}).[10] In particular, this makes the non-radiative relaxations from $^1G_4$ level very unlikely since the nearest level below ($^3F_4$) is ~3000 cm^{-1} apart. That also increases the fluorescence lifetime of $^1G_4$ level which is in favour of energy transfer (b) in Fig. 1.[11–13] Figure 3 shows the emission spectrum of NLF: 0.5% Pr^{3+}, 5% Yb^{3+} excited into $^3P_2$ level at 450 nm. The observed lines mostly correspond to $^3P_0$ level emission of Pr^{3+} . This spectrum corresponds to that found in literature.[14] The spin forbidden transitions from $^1D_2$ level to ^3H_J levels are very weak

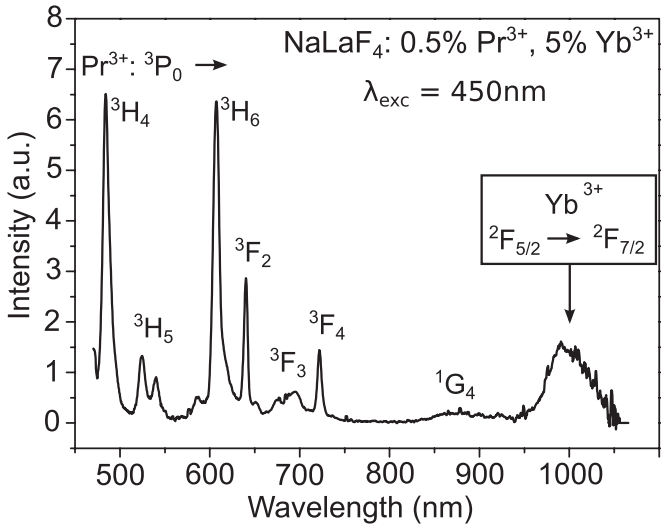

FIG. 3. Emission spectrum of NLF:0.5% Pr^{3+}, 5% Yb^{3+} under excitation into $^3P_2$ level of Pr^{3+} at 450 nm. The emission below 900 nm comes from $^3P_0$ level of Pr^{3+}, and the emission at 1000 nm from $^2F_{5/2}$ level Yb^{3+} (see Fig. 1).

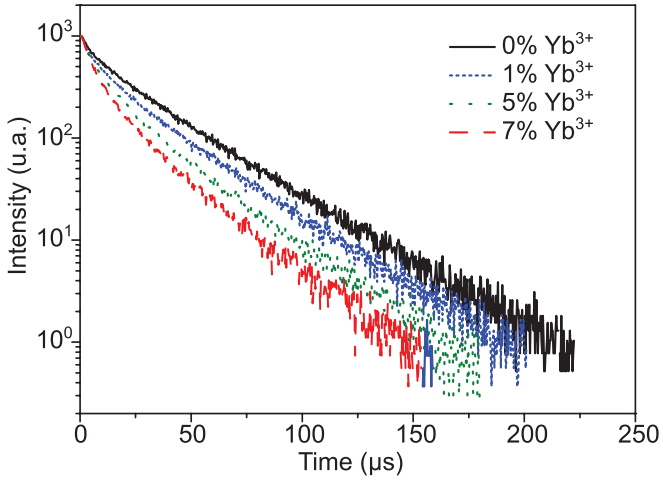

FIG. 4. Fluorescence decay of Pr^{3+} under excitation at 450 nm into $^3P_2$ level recorded at 610 nm corresponding to the transition $^3P_0 \rightarrow {}^3H_6$.

essentially because $^1D_2$ level cannot be non-radiatively populated after an excitation into ^3P_j. This means that the energy transfer (c) in Fig. 1 is very unlikely under excitation into ^3P_j levels which is favourable to an effective quantum cutting for 1 μm emission. On the other hand, the band around 1 μm is due to the emission from $^2F_{5/2}$ level of Yb^{3+}. This shows that, energy transfer between Pr^{3+} and Yb^{3+} occurs. The question is to determine whether quantum-cutting occurs or not.

The fluorescence decay of $^3P_0$ level under excitation into $^3P_2$ level at 450 nm has been recorded in several NLF samples doped with 0.5% Pr^{3+} and x% Yb^{3+} (x = 0, 1, 5, 7) for the emission at 610 nm corresponding to the transition $^3P_0 \rightarrow {}^3H_6$. As it can be seen in Fig. 4, for x = 0 the decay is exponential. As the Yb^{3+} concentration increases, the decay becomes more and more inexponential and the lifetime decreases. The values are gathered in Table I. The average lifetime listed in Table I is calculated by the following formula:

$$\tau = \frac{\int_0^\infty I(t).t.dt}{\int_0^\infty I(t).dt} \quad (1)$$

TABLE I. Lifetime of $^3P_0$ and $^1D_2$ levels of Pr^{3+} and transfer efficiency $Pr^{3+} \rightarrow Yb^{3+}$ in NLF : 0.5% Pr^{3+}, x% Yb^{3+}.

Yb^{3+} (at. %)	$^3P_0$ lifetime (μs)	Transfer efficiency $^3P_0$ (%)
0	29.7	0
1	26.0	13
5	21.4	28
7	18.1	39

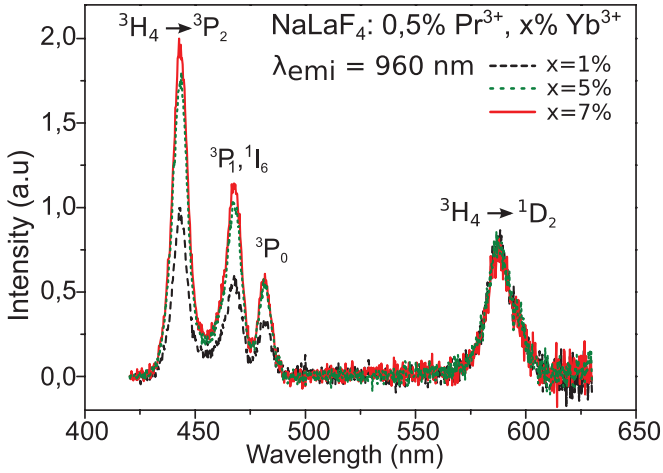

FIG. 5. Excitation spectra of emission at 960 nm of $^2F_{5/2}$ Yb^{3+} level in several samples with a variable Yb^{3+} concentration.

and the transfer efficiency η_x in NLF : 0.5% Pr^{3+}, x% Yb^{3+} with the formula:

$$\eta_x = 1 - \frac{\tau_x}{\tau_0}, \tag{2}$$

where τ_x is the average lifetime of Pr^{3+} in the sample co-doped with 0.5% Pr^{3+}, x% Yb^{3+}, and τ_0 is the lifetime of Pr^{3+} in the sample single doped with 0.5% Pr^{3+}. The transfer probability in the case of dipole-dipole interaction is given by Dexter formula:[15]

$$P_{dd}(R) = \frac{3c^4\hbar^4\sigma_A}{4\pi n^4 \tau_S R^6} \int \frac{f_S(E)F_A(E)}{E^4} dE. \tag{3}$$

Thus, it depends on the distance between donor and acceptor ions and on the overlap integral between the donor emission and the acceptor absorption. The value of this integral does not change when the ions concentration increases, so the transfer probability is only function of distances between ions, i.e., function of ions concentrations. The intensity of excitation bands corresponding to different energy transfers depends on the transfer probabilities and, therefore, varies the same way as a function of ions concentrations whatever the transfer. Thus, if energy transfers occurring after excitation into $^1D_2$ or $^3P_0$ are both only one step energy transfers, the intensity of the corresponding excitation bands should vary the same way when the Yb^{3+} concentration increases. In order to point out the quantum cutting process and to evaluate its efficiency, we have recorded the excitation spectra of several samples by monitoring the emission of Yb^{3+} at 960 nm. At this wavelength we carefully checked that the emission comes mainly from Yb^{3+} $^2F_{5/2}$ and that the contribution from Pr^{3+} $^1G_4$ is negligible. They are depicted in Fig. 5.

The excitation spectrum of Yb^{3+} emission shows a first band between 580 nm and 610 nm which corresponds to excitation through $^1D_2$ level, and three other bands between 440 nm and 500 nm which correspond to excitation through ^3P_j levels of Pr^{3+}. When the sample is excited into the $^1D_2$ level, there are two ways to transfer the energy toward Yb^{3+} ion: either via the transfer (c)

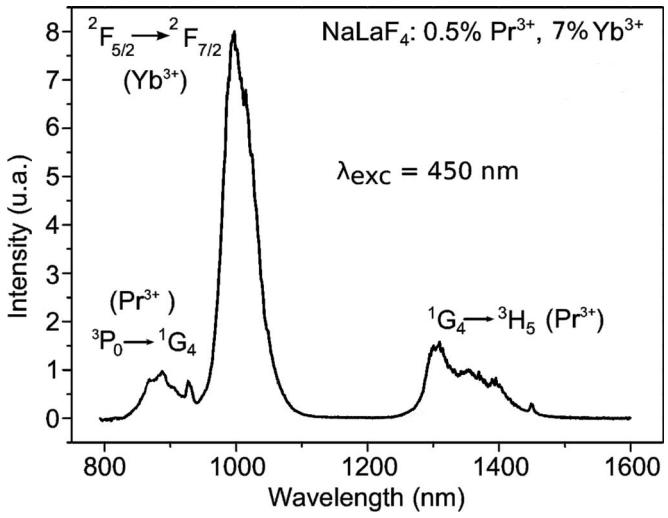

FIG. 6. Infra-red emission spectrum of NLF:0.5% Pr^{3+}, 7% Yb^{3+} under excitation into $^3P_2$ level of Pr^{3+}.

in Fig. 1, or via the transfer (b) in Fig. 1 after the transition $^1D_2 \rightarrow {}^1G_4$ occurred. But in both cases, only one Yb^{3+} ion can be excited. Instead, when the initial excitation populates $^3P_0$ level, two Yb^{3+} ions can be excited; the first one by the cross-relaxation energy transfer (a) in Fig. 1 ($^3P_0$,$^2F_{7/2}$) $\rightarrow$ ($^1G_4$, $^2F_{5/2}$) and the second one by the energy transfer (b) in Fig. 1 ($^1G_4$, $^2F_{7/2}$) $\rightarrow$ ($^3H_4$, $^2F_{5/2}$). To have a chance to observe such a process, each Pr^{3+} ion needs to have at least two Yb^{3+} ions nearby. Indeed, the lifetime of $^2F_{5/2}$ level of Yb^{3+} is longer ($\tau_{^2F_{5/2}} = 935\ \mu s$) than the lifetime of $^1G_4$ level of Pr^{3+} ($\tau_{^1G_4} = 300\ \mu s$). So, to have an efficient transfer (b) in Fig. 1 which occurs necessarily after transfer (a) in Fig. 1, another Yb^{3+} ion in its ground state in the vicinity of Pr^{3+} is needed. If this occurs, the relative intensity of the bands corresponding to the ^3P_j levels in the excitation spectra should increase compare to that of $^1D_2$ band. By normalizing the excitation spectra on the $^1D_2$ band, we can show that quantum cutting effectively occurs for high Yb^{3+} concentrations. The relative intensity in the excitation spectrum of ^3P_j band grows when the concentration increases. For the 7% Yb^{3+} concentration, this intensity is twice the intensity recorded for the 1% Yb^{3+} concentration. This means that there are two times more Yb^{3+} ions excited from $^3P_0$ in that case. Since the first step of energy transfer from $^3P_0$ and from $^1D_2$ should vary the same way, the fact that the intensity doubles for ^3P_j levels means that the second step (energy transfer from $^1G_4$ level) occurs and is as efficient as the first step. At this concentration and for higher Yb^{3+} concentrations, the quantum cutting is very efficient. The efficiency of the first step being 39% (see Table I) the total energy transfer efficiency from $^3P_0$ can be estimate around 78%. Serrano *et al.* show that the efficiency of the first step transfer can reach a value of 97% in KY_3F_{10} for a Yb^{3+} concentration of 20%,[12] so we can hope that by increasing furthermore the concentration we could almost reach a 200% efficiency for quantum cutting process in NLF.

If quantum cutting was the only process existing between Pr^{3+} and Yb^{3+} ions, as it becomes more and more efficient with the increasing of Yb^{3+} concentration, the emission of $^1G_4$ level should vanish because the transfer (b) in Fig. 1 becomes more and more efficient inducing a decrease of the $^1G_4$ population. In Fig. 6, we show emission in the infra-red region for 7 at. % concentration of Yb^{3+}. The emission from $^1G_4$ is clearly seen and is partly due to a back transfer from Yb^{3+}. In order to point out it, we recorded emission spectra of $^1G_4$ level under excitation into Yb^{3+} at 980 nm. In single doped sample with Pr^{3+} no emission from $^1G_4$ is detected, but in double doped samples with Pr^{3+} and Yb^{3+}, an emission around 1.3 μm is detected which corresponds to the Pr^{3+} transition $^1G_4 \rightarrow {}^3H_5$. This clearly demonstrates the back transfer from Yb^{3+} to Pr^{3+}. An example for NLF:0.5% Pr^{3+}, 1% Yb^{3+} is shown in Fig. 7. Unfortunately, when the Yb^{3+} concentration increases this back transfer from Yb^{3+} to Pr^{3+} reduces the emission intensity of Yb^{3+}. Thus, the

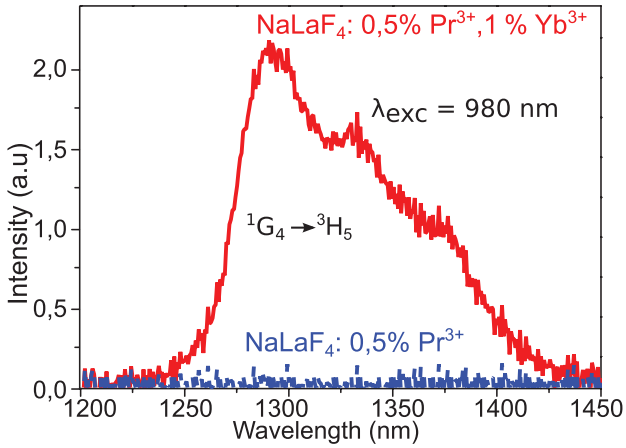

FIG. 7. Infra-red emission spectra of NLF:0.5% Pr^{3+}, 1% Yb^{3+} under excitation into $^2F_{5/2}$ level of Yb^{3+} at 980 nm.

partial quantum efficiency (for wavelength shorter than 1.1 μm which are useful for Si-based solar cells) is also reduced.

In summary, we studied energy transfers in $NaLaF_4$ co-doped with Pr^{3+} and Yb^{3+}. We demonstrated that in Yb^{3+} high concentrated samples quantum-cutting occurs. We analysed precisely the energy transfers involved and we proposed a method to evaluate their respective contributions to Yb^{3+} emission. We also demonstrated that the back-transfer from Yb^{3+} toward the $^1G_4$ level of Pr^{3+} makes that the whole resulting infra-red emission cannot be converted into electron-hole pairs in standard silicon solar cells, limit absorption of which is 1.1 μm, but could be valuable for other types of solar cell materials with smaller energy gap like InN or $In_xGa_{1-x}N$.

This work has been supported by the French Research National Agency (ANR) through Habitat intelligent et solaire photovoltaïque program (project MULTIPHOT-PV No. ANR-09-HABISOL-009). The authors thank the cluster ENERGIES Rhône-Alpes and the "TENERRDIS" pôle de compétitivité for their support.

[1] W. Shockley and H. J. Queisser, J. Appl. Phys. **32**, 510 (1961).
[2] B. S. Richards, Sol. Energy Mater. Sol. Cells **90**, 1189 (2006).
[3] T. Trupke, M. A. Green, and P. Wurfel, J. Appl. Phys. **92**, 1668 (2002).
[4] B. M. van der Ende, L. Aarts, and A. Meijerink, Phys. Chem. Chem. Phys. **11**, 11081 (2009).
[5] X. Huang, S. Han, W. Huang, and X. Liu, Chem. Soc. Rev. **42**, 173 (2013).
[6] Q. Zhang and X. Huang, Prog. Mater. Sci. **55**, 353 (2010).
[7] B. M. van der Ende, L. Aarts, and A. Meijerink, Adv. Mater. **21**, 3073 (2009).
[8] A. Guille, A. Pereira, C. Martinet, and B. Moine, Opt. Lett. **37**, 2280 (2012).
[9] D. Serrano, A. Braud, J.-L. Doualan, P. Camy, and R. Moncorgé, J. Opt. Soc. Am. B **28**, 1760 (2011).
[10] A. Sarakovskis, J. Grube, A. Mishnev, and M. Springis, Opt. Mater. **31**, 1517 (2009).
[11] W. Jordan, A. Jha, M. Lunt, S. Davey, R. Wyatt, and W. Rothwell, J. Non-Cryst. Solids **184**, 5 (1995).
[12] D. Serrano, A. Braud, J.-L. Doualan, P. Camy, A. Benayad, V. Ménard, and R. Moncorgé, Opt. Mater. **33**, 1028 (2011).
[13] Y. G. Choi and J. Heo, J. Non-Cryst. Solids **217**, 199 (1997).
[14] E. van der Kolk, O. T. Kate, J. Wiegman, D. Biner, and K. Krämer, Opt. Mater. **33**, 1024 (2011).
[15] D. L. Dexter, J. Chem. Phys. **21**, 836 (1953).